power levels. Excellent agreement between laboratory measurements and model predictions has been demonstrated. The comparisons were made for signal levels up to where 6 dB of gain compression occurred.

ACKNOWLEDGMENT

The authors wish to thank Dr. B. E. Spielman, R. E. Neidert, and B. Sheleg for helpful comments and suggestions. We also thank H. Heddings for his assistance in the laboratory measurements.

REFERENCES

[1] H. A. Willing and P. de Santis, "Modeling of Gunn domain effects in GaAs MESFET's," *Inst. Elec. Eng. Electron. Lett.*, vol. 13, no. 18, pp. 537–539, 1977.
[2] K. Lehovec and R. Zuleeg, "Voltage-current characteristics of GaAs J-FET's in the hot electron range," *Inst. Elec. Eng. Solid-State Electron.*, vol. 13, pp. 1415–1429, 1970.
[3] R. W. H. Engelmann and C. A. Liechti, "Gunn domain formation in the saturated region of the GaAs MESFET's," in *IEEE Int. Electron Devices Conf. Digest*, 1976, pp. 351–354.
[4] R. S. Tucker and C. Rauscher, "Modeling the 3rd-order intermodulation-distortion properties of a GaAs FET," Electron. Lett., vol. 13, no. 17, pp. 508–510, 1977.

Surface-Oriented Transferred-Electron Devices

MICHAEL S. SHUR AND LESTER F. EASTMAN, FELLOW, IEEE

Abstract—**The application of MESFET technology to the manufacturing of surface-oriented transferred-electron devices (TED's) with parameters close to GaAs MESFET's is discussed. The limitations related to the contact resistance, fringing capacitance, domain formation time, impact ionization, and heat sinking are analyzed for GaAs and InP devices. Our estimates show that the surface-oriented devices can be used as microwave LSA generators at higher frequencies than the conventional LSA diodes. In a domain mode, the surface-oriented TED's can yield low values of the power-delay product comparable to those of GaAs MESFET's at higher speeds. The analysis of impact ionization within a high-field domain leads to a conclusion that even InP logic devices with practical lengths of the active layer can be manufactured with doping densities up to $10^{17}cm^{-3}$. The estimate of the temperature rise indicates that a CW operation is possible for practical device parameters. Because the parameters of surface-oriented TED's are similar to those of GaAs MESFET's they may be manufactured using the rapidly developing GaAs integrated-circuit technology and used in combination with GaAs MESFET's.**

I. INTRODUCTION

THE ADVANTAGES of GaAs MESFET's compared to Gunn devices may be partially related to a better technology and to a planar construction which provides better heat sinking. This technology now may be applied to manufacture surface-oriented Gunn devices (gateless FET's). Such devices have much in common with planar Gunn devices which have been extensively studied previously (see, for example, [1]-[6]) but their parameters, such as a very high doping density (up to $10^{17}cm^{-3}$), the small thickness of the active layer (up to 0.15 μm), the large ratio of the active layer length over the thickness, etc., are close to the parameters of GaAs MESFET's. The surface-oriented MESFET's can be used as millimeter-wave generators and also as the components of monolithic GaAs integrated circuits where the combination of transferred-electron devices (TED's) and FET's proved to be especially effective [7].

In this paper we analyze the limitations of surface-oriented TED's related to the device physics and technology. We first derive the criteria of the LSA operation of the surface oriented TED's. It is followed by the estimate of a minimum switching time and a power-delay product in the domain mode and by the consideration of the limitations imposed by the impact ionization within the high-field domain. This calculation is relevant to the possible logic application of the devices. Finally, we consider a heat-sinking problem and derive a simple criterion which has to be fulfilled for a CW operation of the surface-oriented TED's.

II. FREQUENCY LIMITATIONS FOR SURFACE-ORIENTED GUNN GENERATORS

Our approach is similar to the one we used in [8] where we estimated the maximal frequency of generation for regular TED's. Our estimates are based on the simplest equivalent circuit shown in Fig. 1. Here R_c is a contact resistance, R_- is the equivalent negative resistance, and C is the equivalent capacitance. We calculated R_-/R_0 in [8]:

Manuscript received May 25, 1978; revised August 14, 1978.
M. S. Shur is with the School of Engineering, Oakland University, Rochester, MI 48063.
L. F. Eastman is with the School of Electrical Engineering, Cornell University, Philips Hall, Ithaca, NY 14853.

0018-9480/78/1200-1023$00.75 ©1978 IEEE

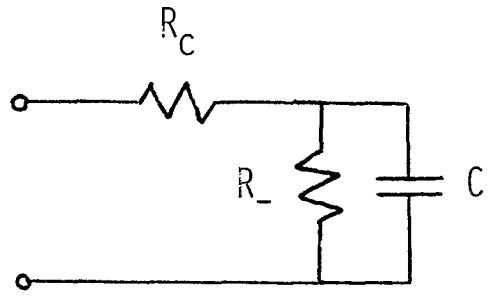

Fig. 1. Simplified equivalent circuit of TED's.

$$\frac{R_-}{R_0} = -\frac{\mu_0 E_0^{3/2}}{v_t(1-r)(E_v)^{1/2}}\frac{\pi}{2^{3/2}} \tag{1}$$

where μ_0 is the low-field mobility, $E_0 = V_0/L$ is the bias field, L is the length of the device, v_t is the peak electron velocity, and E_v is the field of the velocity saturation. This expression is valid when $E_0 > E_v$, but it could be used as an extrapolation for smaller values of E_0.

For regular LSA Gunn generators, C can be estimated as the geometric capacitance C_0 of the device. For surface-oriented LSA TED's the fringing capacitance C_f is more important:

$$C = C_0 + C_f \tag{2}$$

where

$$C_0 = \frac{\epsilon_0 \epsilon h w}{L}.$$

Here $\epsilon_0\epsilon$ is the permittivity, h is the thickness of the active layer, and w is the transverse dimension of the device. According to [9]

$$C_f = 1.5\epsilon_0 \epsilon w \tag{3}$$

so that for surface-oriented devices

$$C_f/C_0 \simeq 1.5L/h \gg 1.$$

The edge contact resistance

$$R_c \simeq 2/(\sigma w) \tag{4}$$

where σ is the low-field conductivity.

Using (1)–(4) we can estimate the cutoff frequency for the circuit shown in Fig. 1 as in [8].

$$f_c \simeq \frac{1}{2\pi C(|R_-|R_c)^{1/2}} = \frac{2^{1/4}(1-r)^{1/2}}{3\pi^{3/2}}\left(\frac{h}{L}\right)^{1/2}\frac{v_t^{1/2}E_v^{1/4}}{\mu_0^{1/2}E_0^{3/4}}\frac{\sigma}{\epsilon_0\epsilon}. \tag{5}$$

As can be seen from (5), the cutoff frequency generators are equal to a small fraction of the inverse dielectric relaxation time. The criterion $f < f_c$ where f is the frequency of generation leads to the following condition:

$$\frac{n_0}{f} > \frac{3\pi^{3/2}}{2^{1/4}}\cdot\frac{\epsilon_0\epsilon E_t^{1/2}}{q(\mu_0)^{1/2}v_t^{1/2}}\cdot\left(\frac{L}{h}\right)^{1/2} \cdot\left(\frac{E_t}{E_v}\right)^{1/4}\left(\frac{E_0}{E_t}\right)^{3/4}\frac{1}{(1-r)^{1/2}}. \tag{6}$$

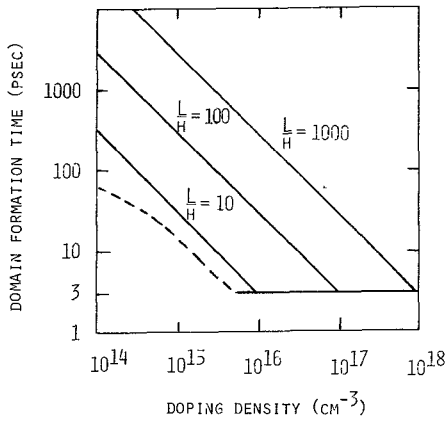

Fig. 2. Domain formation time versus doping density for GaAs TED's. Dashed line: regular TED's. Solid lines: surface-oriented TED's.

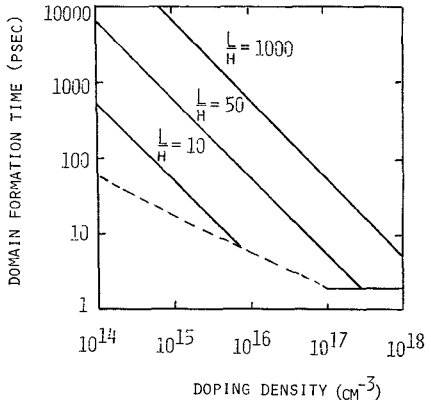

Fig. 3. Domain formation time versus doping density for InP TED's. Dashed line: regular TED's ($L = 10$ μm). Solid line: surface-oriented TED's.

Assuming $\epsilon = 12.9$, $\mu = 0.8$ m^2/V·s, $v_t = 2.10^5$ m/s, $E_t = 3.5$ kV/cm, $E_v = 10$ kV/cm, $E_0 = 10$ kV/cm, and $r = 1/2$ for GaAs, and $\mu = 0.4$ m^2/V·s, $v_t \backsim 2.5$ 10^5 m/s, $E_t \simeq 10$ kV/cm, $\epsilon = 12.4$, $E_v \simeq 30$ kV/cm, $E_0 \simeq 30$ kV/cm, and $r = 0.24$, for InP, we find for GaAs and InP, respectively,

$$\frac{n_0(cm^{-3})}{f(\text{GHz})} > 3.5\cdot 10^{13}\left(\frac{L}{h}\right)^{1/2} \tag{6a}$$

$$\frac{n_0(cm^{-3})}{f(\text{GHz})} > 6.10^{13}\left(\frac{L}{h}\right)^{1/2}. \tag{6b}$$

These criteria are more stringent than for the regular TED's [8]. The physical reason for this difference is a comparatively large value for the fringing capacitance which, in turn, is due to the fact that the stray electric field is not limited to the active area but penetrates into a substrate where the electrostatic energy is now stored. On the other hand, the same effect leads to a larger domain formation time τ_f and to a smaller minimal frequency of the LSA operation:

$$f_{\min} \simeq \frac{1}{2\pi\tau_f}. \tag{7}$$

We can estimate τ_f as follows [10], [11]:

$$\tau_f \simeq 3C_D R_0 \tag{8}$$

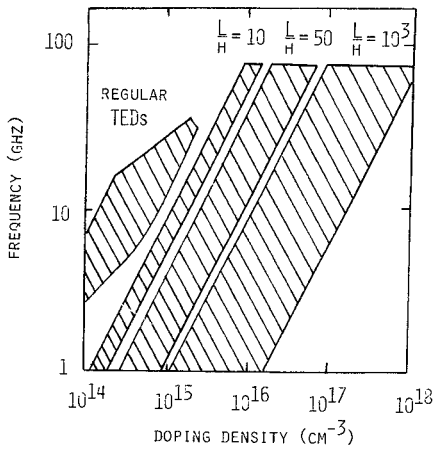

Fig. 4. Frequency regions of possible LSA operation (dashed) for regular ($L=10$ μm) and surface-oriented GaAs TED's.

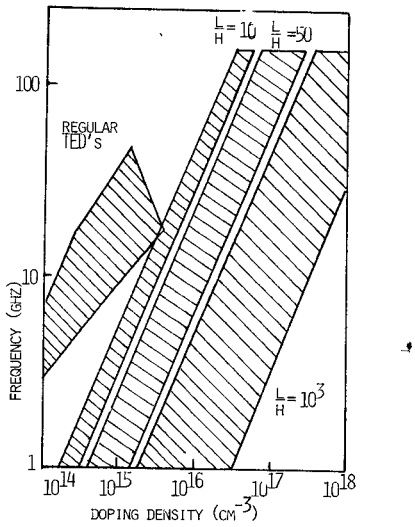

Fig. 5. Frequency regions of possible LSA operation (dashed) for regular ($L=10$ μm) and surface-oriented InP TED's.

where C_D is the domain capacitance. For surface-oriented devices [11]

$$C_D \simeq \frac{\epsilon_0 \epsilon W h}{d} + \epsilon_0 \epsilon W \simeq \epsilon_0 \epsilon W \tag{9}$$

where the first term represents a regular domain capacitance (d is the effective domain width) and the second term is due to the fringing capacitance. The first term is negligibly small because we assume that $d \gg h$. From (8) and (9) we have

$$\tau_f \simeq 3 \frac{L}{h} \frac{\epsilon_0 \epsilon}{\sigma} = 3 \frac{L}{h} \frac{\epsilon_0 \epsilon}{q n_0 \mu_0}. \tag{10}$$

The dependences τ_f versus n_0 for regular and surface-oriented TED's are shown in Figs. 2 and 3 for GaAs and InP, respectively. We also take into account that τ_f cannot be smaller than the electron energy relaxation time τ_T ($\sim 2 \div 3$ ps for GaAs and $\simeq 1 \div 2$ ps for InP), as indicated by the horizontal solid lines in Figs. 2 and 3. The domain formation time for regular TED's was calculated in the frame of theory developed in [10].

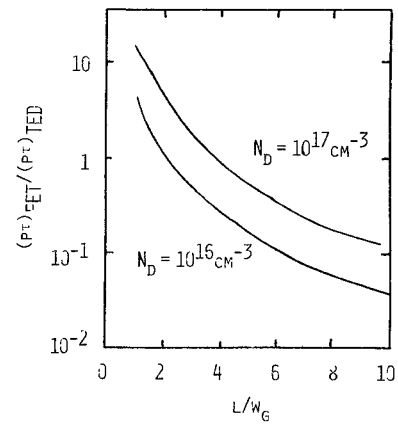

Fig. 6. Comparison of power-delay products for GaAs MESFET's and surface-oriented TED's. N_D is the doping density for MESFET's.

The frequency regions of the LSA operation for GaAs and InP are shown in Figs. 4 and 5. For surface-oriented TED's the boundaries of the regions are determined by (6) and (7) and by the the condition $f < 1/2\pi\tau_T$. The regions shown for regular TED's are for diodes with $L = 10^{-3}$ cm and $W = 5.10^{-2}$ cm as shown in [8, Fig. 5]. For surface-oriented TED's, skin-effect limitations (which are so crucial for regular TED's) are not important because of the very small thickness of the active layers. This is why we could expect to generate higher frequencies using surface-oriented TED's. The frequency limits considered above could be changed if the dielectric passivation layer is used. It follows from (6) and (8) that both f_c and f_{min} are proportional to $(1+\epsilon_r/\epsilon)^{-1}$ where ϵ_r and ϵ are the dielectric constants of the dielectric layer and GaAs, respectively.

III. Switching Time and Power-Delay Product

The switching time of the surface-oriented TED's is determined by the domain formation time as shown in (10) and Figs. 2 and 3. The required power

$$P = q n_0 \mu E_s \cdot h \cdot W \cdot E_0 L = \frac{3 \epsilon_0 \epsilon E_0 E_s L^2 W}{\tau_f}. \tag{11}$$

We could compare this expression with a similar expression for GaAs MESFET's that we derived in [12]:

$$P_{FET} = \frac{W_G^2 W E_s (2 \epsilon_0 \epsilon q N_D (V_{Bi} - V_G))^{1/2}}{\tau_{FET}}. \tag{12}$$

Here P_{FET} and τ_{FET} are the power and switching time for a GaAs MESFET, V_{Bi} is the built-in voltage, V_G is the gate voltage, W_G is the gate length, and W is the device width.

$$\frac{P_{FET} \tau_{FET}}{P \tau_f} \simeq \frac{2^{1/2}}{3} \left(\frac{W_G}{L} \right)^2 \left(\frac{q N_D (V_{Bi} - V_G)}{\epsilon_0 \epsilon E_0^2} \right)^{1/2}$$

$$\simeq 12.5 \left(\frac{N_D}{10^{17}} \right)^{1/2} \left(\frac{W_G}{L} \right)^2. \tag{13}$$

Here we assumed $E_0 \simeq 4$ kV/cm, $V_{B_1} = 0.8$ V, and $V_G = 0$. One can see that short surface-oriented TED's can yield the low values of the power-delay product comparable to those for GaAs MESFET's with a doping density $N_D \backsim 10^{17}$ cm^{-3} (see Fig. 6) and a higher speed.

IV. The Impact Ionization Within a High-Field Domain

The impact ionization within a high-field domain may become a problem in long high-doped TED's when the domain field E_m exceeds the critical breakdown field E_b, i.e.,

$$U_d > U_{db} \tag{14}$$

where U_d is the domain voltage and U_{db} is the domain breakdown voltage such that E_m is equal to E_b. As shown in [13], the domain voltage and the domain field are related as follows.

$$U_d = \frac{\epsilon_0 \epsilon E_m^2}{q n_0} \cdot F\left(\frac{n_0}{n_{cr}}\right). \tag{15}$$

Here n_{cr} is the characteristic electron concentration that depends on the shape of the electron drift velocity $v(E)$ and diffusion $D(E)$ versus electric field curves[1].

The F versus n_0/n_{cr} dependence is shown in Fig. 7. It is universal and does not depend on the material parameters. If $n_0/n_{cr} \ll 1$,

$$F\left(\frac{n_0}{n_{cr}}\right) \simeq 1/2.$$

If $n_0/n_{cr} \gg 1$,

$$F\left(\frac{n_0}{n_{cr}}\right) \simeq \frac{4\sqrt{2}}{3}\left(\frac{n_0}{n_{cr}}\right)^{1/2}.$$

These two expressions agree with the results of the analytical theory of the high-field domains developed in [14], [15].

As shown in [13] for

$$0.01 < \frac{n_0}{n_{cr}} < 10^3$$

we have

$$\left(\frac{n_0}{n_{cr}}\right) \simeq 0.363 + 1.67\left(\frac{n_0}{n_{cr}}\right)^{1/2}. \tag{16}$$

At the threshold field the domain voltage U_d is equal to

$$U_d = (E_t - E_s)L \tag{17}$$

where E_t is the electron peak velocity field and E_s is the domain sustaining field.

Using (13), (14), (16), and (17) we find that the parameters of a TED must satisfy the following criterion:

[1]In [13] we used the approximation of the field-independent diffusion. One can show, however, that the same result is valid also for the field-dependent diffusion though in this case the value of n_{cr} has to be modified.

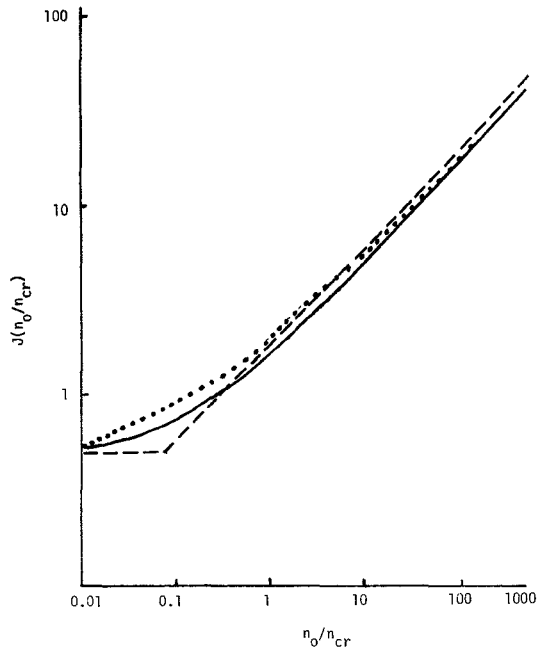

Fig. 7. F versus n_0/n_{cr} [13]. Solid line: computer calculation. Dashed lines: analytical approximations valid for small and large n_0/n_{cr} values. Dotted line: analytical approximation valid for $0.01 < n_0/n_{cr} < 1000$, as in (13).

$$\frac{n_0 L}{0.363 + 1.67\left(\frac{n_0}{n_{cr}}\right)^{1/2}} < \frac{\epsilon_0 \epsilon E_b 2}{q(E_t - E_s)}. \tag{18}$$

Otherwise, the breakdown would occur at the threshold. The following parameters are typical for high-doped GaAs and InP, respectively.

$$\epsilon \simeq 12.9 \quad E_t - E_s \backsim 2.3 \text{ kV/cm}$$
$$n_{cr} \backsim 2.9 \cdot 10^{15} \text{ cm}^{-3} \quad E_b \backsim 150 \text{ kV/cm}$$

and

$$\epsilon \simeq 12.4 \quad E_t - E_s \backsim 9.3 \text{ kV/cm}$$
$$n_{cr} \backsim 5 \cdot 10^{16} \text{ cm}^{-3} \quad E_b \backsim 180 \text{ kV/cm}.$$

As mentioned above the values of n_{cr} are dependent on the shape of $V(E)$ and $D(E)$ and also on the low-field mobility. The detailed calculations of n_{cr} for GaAs and InP will be published elsewhere. The values of n_{cr} given above are for GaAs with the low-field mobility about 6000 cm^2/s and for InP with the low-field mobility about 3100 cm^2/V·s. The relatively low values of E_b we have assumed are typical for the breakdown within a traveling domain where the breakdown field is smaller because of the accumulation of the electron-hole pairs from cycle to cycle [16]. We also assumed a higher breakdown field for InP in spite of a smaller band gap based on the results of the preliminary measurements of the breakdown voltage in InP. For the parameters given above, we find from (18) for GaAs and InP, respectively,

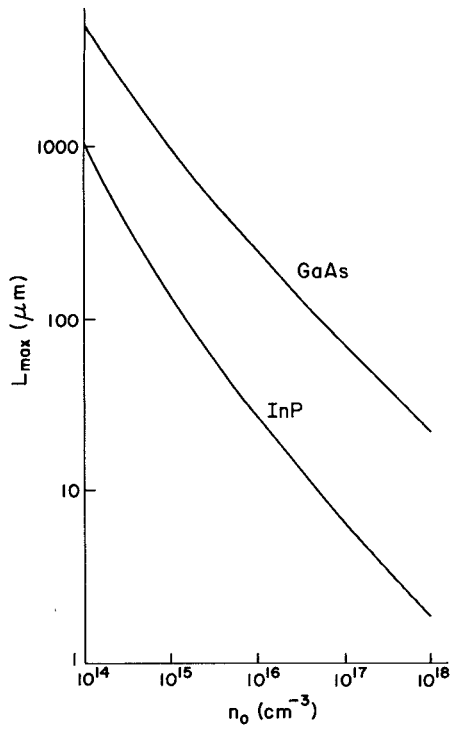

Fig. 8. Doping-length limitations related to impact ionization within a high-field domain at the threshold voltage.

$$L_{max}(\mu m) \leqslant \frac{2.53 \cdot 10^{17}}{n_0(cm^{-3})} + \left(\frac{4.66 \cdot 10^{20}}{n_0(cm^{-3})} \right)^{1/2} \quad (19)$$

$$L_{max}(\mu m) < \frac{0.868 \cdot 10^{17}}{n_0(cm^{-3})} + \left(\frac{3.19 \cdot 10^{18}}{n_0} \right)^{1/2}. \quad (20)$$

Equation (19) is similar to the estimate given in [19], but (20) is different because of the higher breakdown field assumed. As can be seen from (19) and (20) and Fig. 8, the limitations imposed by the impact ionization are considerably more stringent in InP.

V. Heat-Sinking Considerations

Surface-oriented TED geometry is shown in Fig. 9. We can assume that the heat flow is perpendicular to the buffer layer and to the substrate. The temperature distribution $T(x)$ is described by the equations of heat conduction:

$$\frac{d}{dx} K_a \frac{dT}{dx} = -Q \quad (21)$$

for the active layer, and

$$\frac{d}{dx} K_s \frac{dT}{dx} = 0 \quad (22)$$

for the buffer layer and for the substrate. Here $K_a = \alpha_a / T$ and $K_s = \alpha_s / T$ are heat conductivities for the active layer and the buffer and substrate, respectively, and

$$Q \backsim q n_0 v_s E_0$$

is the heat generation density.

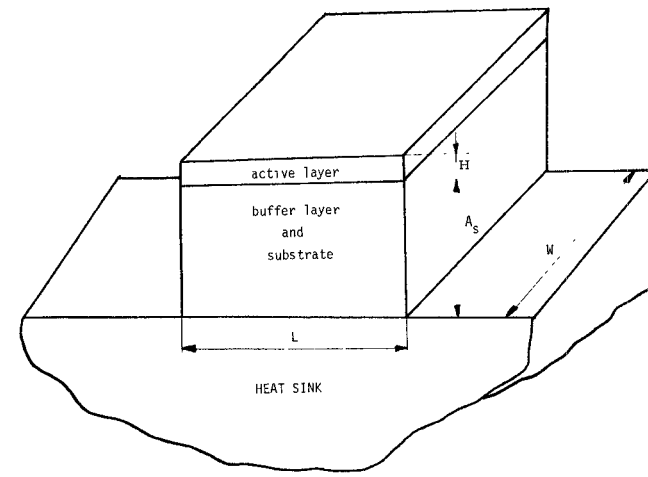

Fig. 9. Surface-oriented TED geometry.

A maximum temperature T_m which is reached at the surface of the active layer is given by the following expression [17]:

$$T_{max} = \left[T_0 + \frac{\gamma Q h (Lw)^{1/2}}{(2\pi)^{1/2} K_m} \right] \exp \frac{Qh^2}{2\alpha_a} + \frac{QhA_s}{\alpha_s}. \quad (23)$$

Here T_0 is the ambient temperature, K_m is the heat conductivity of the heat sink, and γ is a numerical coefficient which depends on the L/w ratio (γ is about 1 by the order of magnitude). If $Qh^2/2\alpha_a < 1$ and $QhA_s/\alpha_s < 1$ (the estimates for typical parameters of MESFET's and surface-oriented TED's show that these unequalities are fulfilled) and, furthermore, the temperature drop in the heat sink (see the second term in the parenthesis in (23)) is small compared to the ambient temperature T_0, (23) can be simplified:

$$T_{max} \backsim T_0 + \frac{QhA_s}{K_{s0}} \quad (24)$$

where

$$K_{s0} = \frac{\alpha_s}{T_0}.$$

Here we have assumed that $A_s \gg h$. The temperature increase

$$\Delta T = T_{max} - T_0$$

should be less than the critical value ΔT_{cr}. That leads to the following criterion:

$$\frac{E_0}{E_t} n_0 h A_s < \frac{T_{cr} K_{s0}}{q v_s E_t}. \quad (25)$$

Assuming $K_{s0} \backsim 54$ W/m·grad, $v_s \simeq 0.85 \cdot 10^5$ m/s, and $E_t \backsim 3.6$ kV/cm for GaAs, and $K_{s0} \backsim 70$ W/m·grad, $V_s = 0.7 \cdot 10^5$ m/s, and $E_t \backsim 11$ kV/cm for InP, and $\Delta T_{cr} \simeq 250$ K, we get

$$\frac{E_0}{E_t} n_0(cm^{-3}) h(cm) A_s(cm) \leqslant 2.92 \cdot 10^{10}(cm^{-1})$$

for GaAs, and

$$\frac{E_0}{E_t} n_0(\mathrm{cm}^{-3}) h(\mathrm{cm}) A_s(\mathrm{cm}) \leqslant 1.42 \cdot 10^{10}(\mathrm{cm}^{-1})$$

for InP. Though these criteria could be met, they are rather stringent for high-doped devices so that the pulse operation should be considered.

If the pulse width τ_p is larger than the characteristic time of the temperature rise

$$\tau_T \backsim \frac{A_s^2 \cdot \rho c}{K_s}$$

the thermal equilibrium will be established by the end of the pulse. Here ρ is the density and c is the specific heat. Assuming $\rho \simeq 5.37 \cdot 10^3$ kg/m^3 and $c \approx 317$ J/kg·grad for GaAs, we get

$$\tau_T(\mathrm{s}) \simeq 3.15 \cdot 10^{-8} \cdot A_s^2(\mu\mathrm{m}).$$

For short pulses $\tau_p < \tau_T$, we have

$$T_{\max} \simeq T_0 + \frac{Q\tau_p}{\rho s}. \tag{26}$$

In this case, assuming that the temperature increase should be less than the critical value ΔT_{cr}, we get [18]

$$n_0 \frac{E_0}{E_t} \tau_p < \frac{\Delta T_{cr} \rho c}{q U_s E_t}. \tag{27}$$

For the values of the parameters given above, we find for GaAs

$$n_0(\mathrm{cm}^{-3}) \frac{E_0}{E_t} \cdot \tau_p(\mathrm{s}) \leqslant 8.7 \cdot 10^{10}(\mathrm{cm}^{-3} \cdot \mathrm{s}). \tag{28}$$

VI. Conclusion

Our estimates show that the GaAs and InP surface-oriented TED's can be used as microwave LSA generators at higher frequencies than the conventional LSA diodes. The physical reason is that for very thin active layers the skin-effect limitations are not important. In a domain mode, these devices may be used for logic application. They can yield low values of power-delay products comparable to those for GaAs MESFET's at higher speed. InP devices have a higher maximum frequency and a smaller switching time than GaAs devices. The impact ionization within a high-field domain limits the possible values of the doping density and active layer length for the logic applications. But even for InP where this limitation is more stringent, practical devices can be manufactured with the doping density up to 10^{17} cm^{-3}. The derived criterion of a CW operation shows that such an operation is possible for practical device parameters. Because the parameters of surface-oriented TED's are close to those of GaAs MESFET's, they may be manufactured using the developing GaAs integrated-circuit technology and effectively used in combination with GaAs MESFET's.

References

[1] R. Becker and B. G. Bosch, "Power-frequency limitations of planar-type GaAs transferred electron devices," in *Proc. Third Int. Symp. Gallium Arsenide and Related Compounds*, (The Institute of Physics Conf., Series No. 9), 1970, pp. 163–171.

[2] K. Sekido, M. Takeuchi, F. Hasegawa, and Y. Hayakawa, "Fabrication of planar-type GaAs bulk effect pulse devices," *NEC Res. Dev.*, no. 18, pp. 106, July 1970.

[3] K. H. Bachem, J. Engelmann, and K. Heime, "Completely planar Gunn-effect devices," in *Proc. 5th Conf. on Solid-State Devices*, Tokyo, Japan, 1973.

[4] T. Sugeta, M. Tanimoto, T. Ikoma, and H. Yanai, "Characteristics and applications of a Schottky-barrier-gate Gunn-effect digital device," *IEEE Trans. Electron Devices*, vol. ED-21, pp. 504–515, Aug. 1974.

[5] K. Mause, A. Schlachetzki, E. Nesse, and H. Salow, "Gunn device gigabit rate digital microscircuits," *IEEE J. Solid-State Circuits*, vol. SC-10, pp. 2–12, Feb. 1975.

[6] T. Nakamura, S. Hasuo, and G. Goto, "Gunn-effect functional devices," *Fujitsu Sci. Tech. J.*, vol. 11, no. 1, pp. 83–106, Mar. 1975.

[7] T. G. Mills, D. H. Claxton, T. M. Crishal, and L. M. Tichauer, "GaAs monolithic integrated circuits and device development," in *Abstracts Sixth Biennial Conf. on Active Microwave Semiconductor Devices and Circuits* (Cornell University, Ithaca, NY), 1977, p. 39.

[8] L. F. Eastman and M. S. Shur, "Frequency limitations of transferred-electron devices related to quality of contacts," *Solid-State Electron.*, vol. 21, pp. 787–791, 1978.

[9] R. W. H. Engelmann and C. A. Liechti, "Gunn domain formation in the saturated current region of GaAs MESFET's," *IEDM Tech. Dig.*, pp. 351–354, Dec. 1976.

[10] M. E. Levinshtein and M. S. Shur, "Transient processes in Gunn diodes," *Solid-State Electron.*, vol. 18, pp. 983–999, 1975.

[11] R. W. H. Engelmann, "Simplified model for the domain dynamics in Gunn effect semiconductors covered with dielectric sheets," *Electron. Lett.*, vol. 4, pp. 546–547, 1968.

[12] M. S. Shur, "Analytical model of GaAs MESFET's," *IEEE Trans. Electron Devices*, vol. ED-25, pp. 612–618, June 1978.

[13] ——, "Maximum electric field in high-field domain," *Electron. Lett.*, accepted for publication.

[14] P. N. Butcher, W. Fawcett, and C. Hilsum, "A simple analysis of stable domain propagation in the Gunn effect," *Brit. J. Appl. Phys.*, vol. 17, no. 7, pp. 841–850, 1967.

[15] B. L. Gelmont and M. S. Shur, "Analytical theory of stable domains in high-doped Gunn diodes," *Electron. Lett.*, vol. 6, no. 12, pp. 385–387, 1970.

[16] B. L. Gelmont and M. S. Shur, "*S*-type current-voltage characteristic in Gunn diodes," *J. Phys. D: Appl. Phys.*, vol. 6, no. 7, pp. 842–850, 1973.

[17] S. Knight, "Heat flow in n^{++}–n–n^{+} epitaxial GaAs bulk devices," in *Proc. IEEE*, vol. 55, 1967.

[18] M. E. Levinshtein, Yu K. Pozhela, and M. S. Shur, "Gunn effect," *Sov. Radio* (Moscow), (in Russian), 1975.